[11] Yang, H., and Saif, M., "Robust Observation and Fault Diagnosis in a Class of Time-Delay Control Systems," *Proceedings of American Control Conference*, Vol. 5, Inst. of Electrical and Electronics Engineers, New York, 1997, pp. 478–482.

[12] Guan, Y., and Saif, M., "A Novel Approach to the Design of Unknown Input Observers," *IEEE Transactions on Automated Control*, Vol. 36, No. 5, 1991, pp. 632–635.

[13] Zoran, G., and Qureshi, M. T. J., *Lyapunov Matrix Equation in System Stability and Control*, Academic, San Diego, 1995, pp. 42–44.

[14] Douglas, R. K., and Speyer, J. L., "Robust Fault Detection Filter Design," *Journal of Guidance, Control, and Dynamics*, Vol. 19, No. 1, 1996, pp. 214–218.

[15] Chung, W. H., and Speyer, J. L., "A Game Theoretic Fault Detection Filter," *IEEE Transactions on Automated Control*, Vol. 43, No. 2, 1998, pp. 143–161.

Band-Limited Actuator and Sensor Selection for Disturbance Rejection

Robert L. Clark*
Duke University, Durham, North Carolina 27708-0300
and
David E. Cox†
NASA Langley Research Center, Hampton, Virginia 23681-0001

Introduction

A METHOD of selecting actuator and sensor locations from a predetermined set of candidate locations based on the Hankel singular values of the controllability and observability Gramian of flexible structures was outlined previously.[1–4] Within the original formulation, the actuator/sensor selection methodology was based entirely on the Hankel singular values of the control path (P_{yu}) for some finite set of modes and some predetermined set of actuators and sensors.[1,2] Later revisions to this method have included a weighting of the Hankel singular values of the control path (P_{yu}) by that of the Hankel singular values of the performance path (P_{zw}) (Refs. 3 and 4). In the most recent application, the disturbance rejection approach to actuator/sensor selection was applied to the piezoceramic aeroelastic response tailoring investigation wind-tunnel model at the NASA Langley Research Center.[4] The results of that study demonstrated a significant advantage to the application of the disturbance rejection approach.

The methodology outlined herein serves as an extension to the disturbance rejection approach with an added metric aimed at robustness with respect to out-of-bandwidth response. Although the method proposed by Lim[3] determines the actuators and sensors that couple best to modes present in the disturbance path, there is no penalty associated with coupling to higher-order modes that are out of the desired bandwidth for control. All practical realizations of control systems are implemented over some finite bandwidth, and for digital realizations, bandwidth limitations are typically imposed by the computational speed of the digital signal processor and the number of modes within the desired bandwidth. Accurate models of the dynamics within the desired bandwidth for control are required; however, model fidelity typically suffers beyond the identified bandwidth. This is particularly true for distributed parameter systems that have infinite dimensional theoretical models. As a result, compensators that incorporate a roll-off are desired and low-pass filters are frequently used in practice to attenuate the response at higher frequency. The response of out-of-bandwidth modes can lead to spillover and stability issues, particularly in the presence of "aggressive" controllers. However, the best method of attenuating the response out of the desired bandwidth is to have poor observability and/or controllability of such modes as an intrinsic property of the open-loop plant. The proposed approach thus serves to simplify robust controller design in the mitigation of spillover.

To this end, an additional metric is introduced for the selection of actuators and sensors for disturbance rejection. Within the bandwidth of desired performance, a metric consistent with that outlined by Lim[3] is computed to determine the actuators and sensors that couple best for disturbance rejection. However, out of the desired bandwidth, a metric is introduced that penalizes the coupling of actuators and sensors to out-of-bandwidth modes. A combination of the two metrics leads to a tradeoff between performance and robustness to spillover effects in the actuator/sensor selection methodology.

The methodology proposed is outlined in the subsequent section. Following the introduction of the new metric, an analytical example based on a structural acoustic control problem is presented. Conclusions are drawn from the results.

Band-Limited Placement Metric for Disturbance Rejection

The problem of interest is the control of a standard two-port system, as shown in Fig. 1. The upper transfer function $P_{zw}(s)$ represents the path from disturbances $w(s)$ to a measure of the closed-loop system performance $z(s)$. This path is determined by the definition of the active control problem, with tradeoffs that reflect available resources, e.g., control energy, or robustness requirements. The lower transfer function $P_{yu}(s)$ represents the path from the control inputs $u(s)$ to the measured outputs $y(s)$ and is a function of the choice and placement of actuators and sensors, respectively, for the control system. Although usually taken as a given for control design, often there is freedom determining sensor and actuator locations, yielding a design decision that impacts the closed-loop performance. Good placement for control design can be determined from the influence of transducers on the open-loop system's controllability and observability, measured in terms of the Hankel singular values.

As noted by Lim,[3] the Hankel singular values (HSVs) from the disturbance to performance outputs illustrated in Fig. 1 are denoted as

$$\Gamma_{zw}^2 = \text{diag}\left(\gamma_{zw1}^2, \ldots, \gamma_{zwn}^2\right) \tag{1}$$

where Γ_{zw}^2 is a diagonal matrix of the n HSVs of the system. The HSVs provide a measure of the degree of coupling of each of the n modes associated with the performance path of the plant $P_{zw}(s)$. The HSV for each of the pth actuators and qth sensors of the control path can be defined as

$$\Gamma_{y_q u_p}^2 = \text{diag}\left(\gamma_{y_q u_p 1}^2, \ldots, \gamma_{y_q u_p n}^2\right) \tag{2}$$

A baseline reference of HSVs for all p actuators and q sensors is defined as

$$\bar{\Gamma}_{yu}^2 = \text{diag}\left(\bar{\gamma}_{yu1}^2, \ldots, \bar{\gamma}_{yun}^2\right) \tag{3}$$

The placement metric for disturbance rejection, as outlined by Lim,[3] can be expressed as follows for the qth sensor and pth actuator:

$$J_{qp} = \sum_{i=1}^{n} \left(\frac{\gamma_{y_q u_p i}^4}{\bar{\gamma}_{yui}^4} \right) \gamma_{zwi}^4 \tag{4}$$

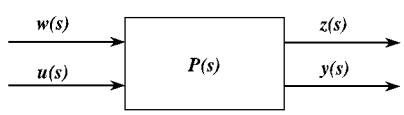

Fig. 1 Block diagram of the two-port design model.

Received 13 November 1998; revision received 29 March 1999; accepted for publication 30 March 1999.

*Associate Professor, Department of Mechanical Engineering and Materials Science, Box 90300. Member AIAA.

†Research Scientist, Flight Dynamics and Control Division, Building 1268A, Room 1156.

This metric positively weights all coupling to the dynamic modes of the system. If we further distinguish between in-bandwidth modes n_{in} and out-of-bandwidth modes $n_{\text{out}} = n - n_{\text{in}}$, the placement metric for disturbance rejection can be expressed as follows:

$$J_{qp_{\text{in}}} = \sum_{i=1}^{n_{\text{in}}} \left(\frac{\gamma^4_{y_q u_p i}}{\bar{\gamma}^4_{yui}} \right) \gamma^4_{zwi} \tag{5}$$

For added robustness, we prefer to limit the coupling through the control path P_{yu} to the out-of-bandwidth modes. As such, a metric is defined by weighting the normalized HSVs for the control path with themselves and taking the reciprocal of the result to emphasize poor coupling:

$$J_{qp_{\text{out}}} = \left[\sum_{i=n_{\text{in}}+1}^{n} \left(\frac{\gamma^4_{y_q u_p i}}{\bar{\gamma}^4_{yui}} \right) \gamma^4_{y_q u_p i} \right]^{-1} \tag{6}$$

Combining the metric associated with in-bandwidth disturbance rejection by the metric associated with out-of-bandwidth robustness, the following metric for actuator/sensor selection results:

$$\hat{J}_{qp} = \bar{J}_{qp_{\text{in}}} + \bar{J}_{qp_{\text{out}}} \tag{7}$$

where the overbar serves to indicate that the in-bandwidth and out-of-bandwidth metrics have been normalized relative to their maximum entry, and $\hat{J}_{qp}$ is the band-limited metric. Thus, a tradeoff exists in the selection of the actuators and sensors based on those that couple well to modes present in the disturbance path over the desired bandwidth of control and those that couple poorly to modes present in the control path outside of the desired bandwidth of control. Therefore, the optimal sensor/actuator pairings should not only couple strongly at low frequencies, but also roll-off naturally at high frequencies.

Description of a Structural Acoustic Model

In preparation for the design of an experimental test rig for structural acoustic control, the actuator/sensor design methodology was applied to an approximate model of a system to determine the best target locations for the transducers. The test rig was constructed from aluminum, measuring 18 × 16 × 0.1875 in. thick. The boundaries were constructed to approximate that of a simply supported plate, and piezoceramic transducers measuring 6 × 4 × 0.0075 in. thick were available for experimental implementation. The larger piezoceramic patches were selected based on the results of a prior study that demonstrated that large aperture transducers serve as spatial wave number filters and provide greater control over the low-bandwidth modes required for structural acoustic control.[5]

The model of the piezostructure was developed from an assumed modes approach as outlined by Clark et al.[6] Seven target locations for piezoceramic sensors and actuators were studied. As single-input/single-output control was desired for the experiment the best two transducers were sought from the possible set of 49. For simplicity, the mass and stiffness contributions of the transducers were omitted from the analytical model. A schematic diagram of target locations is depicted in Fig. 2. The center coordinates of each patch are indicated by an asteric on the nondimensional schematic of the plate. Additionally, the nondimensional coordinates are provided in Table 1. Only one quadrant of the plate was explored for actuator/sensor placement. The magnitudes of simply supported modal shapes are symmetric about the vertical and horizontal axis and thus

Table 1 Center points of piezoceramic transducers in nondimensional plate coordinates

Transducer	x coordinate	y coordinate
1	0.3	0.3
2	0.4	0.4
3	0.5	0.5
4	0.3	0.5
5	0.4	0.5
6	0.5	0.3
7	0.4	0.3

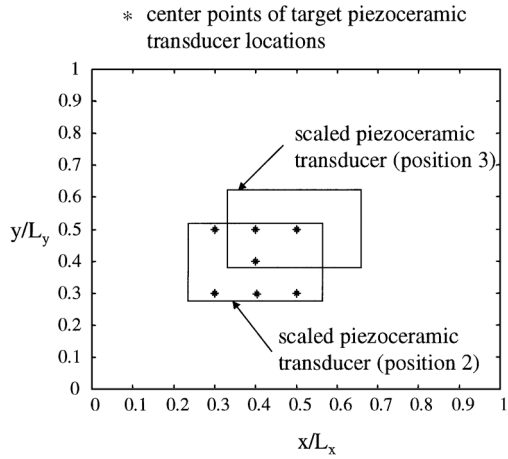

Fig. 2 Schematic of the plate identifying center points of piezoceramic transducers.

coupling strength, which the placement metric measures, are equivalent in the four quadrants. Given that the objective was to reduce the sound power radiated, intuition suggested that a patch centered on the structure and operated as a collocated transducer pair would produce the best result (modes with even indices are inefficient acoustic radiators). Alternative candidate transducer positions were also included along the diagonal of the nondimensional plate as well as on nodal lines of modes with even indices in x and y.

Performance of the closed-loop system is defined in terms of the total power radiated into the far-field. For the purpose of estimating the sound power radiated, the plate was subdivided into 20 rectangular elements having equal surface area. The velocity at the center point of each elemental area was modeled to provide inputs to radiation filters. Assuming that the plate is coupled to a half-space with rigid boundaries, the sound power radiated can be obtained by applying the Rayleigh integral to compute the far-field sound pressure levels in terms of the surface velocity of the vibrating, flexible panel. As detailed by Gibbs et al.,[7] radiation modal expansion can be applied to generate a filter that estimates the sound power radiated in terms of a finite set of discrete velocity outputs. For the purpose of this study, the first radiation mode was used to define the performance path between a generalized force applied uniformly to each mode of the structure and the sound power radiated. The first radiation mode results from a series expansion over all of the structural modes that radiate volumetrically. In developing the radiation filter, a state variable model of the system was constructed. (For greater details on the construction of the piezostructure model and the radiation filter, refer to Ref. 6.)

The model included 60 states for the structural system and 9 states for the radiation filters. A bandwidth of interest was defined below 1200 Hz; thus the first 20 structural states were included in the in-bandwidth computation of the performance metric and the remaining 40 structural states were included in the out-of-bandwidth computation of the performance metric.

Comparison of Actuator/Sensor Selection Strategies

To form a basis of comparison, the proposed strategy for band-limited actuator/sensor selection was compared to the selection strategy outlined in Ref. 4. Limiting the selection to the metric defined in Eq. (4), one obtains the result presented in Fig. 3, which shows the relative merit of all 49 possible SISO transducer paths. As illustrated there is symmetry in the selection because, due to reciprocity, either transducer of a given pair can be used as an actuator or a sensor and result in the same frequency response. For the case presented, the optimal transducer pair is actuator 3 and sensor 3, which corresponds to a single piezoceramic transducer positioned in the center of the plate and operated as a collocated pair. The result of this actuator/sensor selection is consistent with physical intuition because modes with even indices are inefficient acoustic radiators when the structural wave number exceeds the acoustic wave number.

The result obtained with the band-limited actuator/sensor selection strategy for disturbance rejection is distinctly different. Using

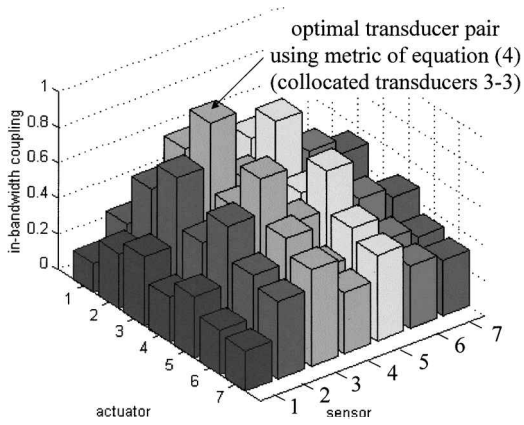

Fig. 3 Barchart of actuator/sensor selection for disturbance rejection outlined in Eq. (4) (Ref. 3).

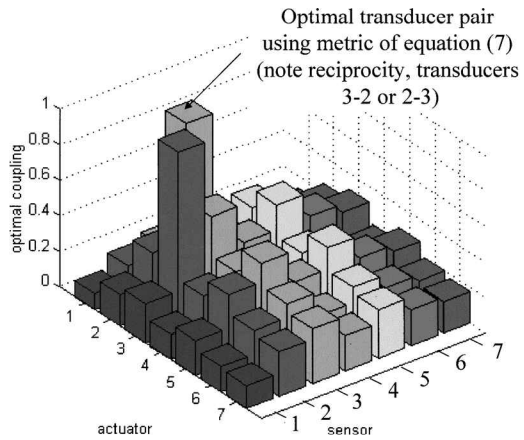

Fig. 4 Barchart of band-limited actuator/sensor selection for disturbance rejection outlined in Eq. (7).

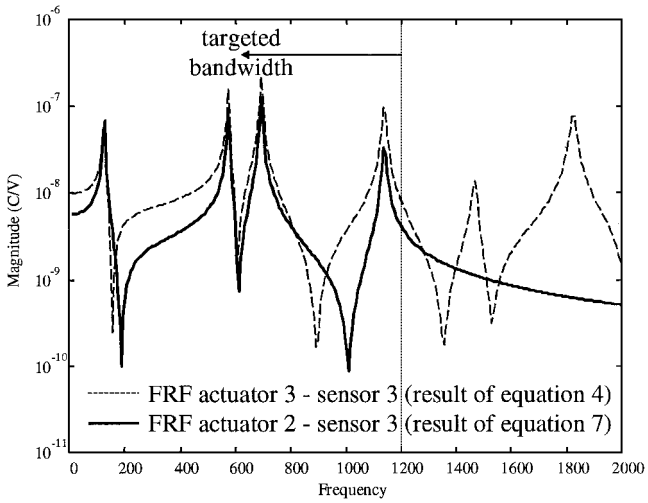

Fig. 5 Magnitude of frequency responses associated with the transducer pairs selected based on Eqs. (4) and (7).

this metric, as outlined in Eq. (7), one obtains the result presented in Fig. 4. For the case studied, the band-limited selection strategy suggests the use of transducer 3 and transducer 2. Again, because of reciprocity one can select either as an actuator or a sensor. This result was nonintuitive, and a schematic diagram of the pair, showing relative position on the structure, is presented in Fig. 2.

Upon comparing the frequency response between the transducer pair resulting from the application of the metric in Eq. (4) and that resulting from the band-limited metric outlined in Eq. (7), one observes that the in-bandwidth (<1200 Hz) response associated with actuator 3 and sensor 3 is slightly greater than that of actuator 2 and sensor 3, as illustrated in Fig. 5. Also note that neither transducer pairs observe or control the (1, 2) or (2, 1) modes of the structure, noted by the absence of resonances corresponding to these modes. As noted in the previous section, the (1, 2), (2, 1), and (2, 2) modes are inefficient acoustic radiators at low frequency and thus are absent from the chosen performance path. Comparing the out-of-bandwidth response of the two transducer options in Fig. 5, one observes that the actuator/sensor pair selected including the band-limited metric results in significantly less response out of the bandwidth of interest (>1200 Hz). Thus, the response of modes outside of the desired bandwidth of operation, which typically lead to stability issues, are suppressed.

Closed-Loop Results

To demonstrate the effect of actuator/sensor selection on closed-loop response, compensators were designed for the best transducers using both metrics, and the resulting closed-loop performance was compared. The analytical plant model had 60 structural states that represented plate dynamics up to about 5000 Hz. The compensators, however, were designed on a reduced-order model that contained only 20 structural states. This reduced-order model is representative of the type of model that would result from experimental system identification.

Linear quadratic Gaussian (LQG) compensators were designed under the model structure of Fig. 1 with control effort penalty of $R = 5 \times 10^{-5}$ (1/V), sensor noise of $V = 1.5 \times 10^{-8}$ (C), and unity process noise and performance weight. The sensor noise was selected to be comparable to the effect of process noise at the frequency where the controller should begin to roll off. Because the piezoceramic element centered on the plate was used as a sensor in both cases, this sensor noise was consistent for both designs. A comparison of the measured output because of unit norm process noise and unit norm sensor noise is shown in Fig. 6.

The control effort penalty was decreased until the closed-loop system, based on the full-order model, was at the border of instability for the collocated actuator/sensor selected by the metric defined in Eq. (4). Applying the same control effort penalty, sensor noise, and process noise, however, for the transducer pair selected from the metric of Eq. (7) resulted in a stable closed-loop response.

The closed-loop responses for each transducer pair are presented in Fig. 7. The response below 1200 Hz is essentially the same for each of the resulting transducer pairs. However, above 1200 Hz, the actuator 3/sensor 3 pair chosen based on the performance metric defined in Eq. (4) results in an unstable response at approximately 1838 Hz. However, the actuator 2/sensor 3 pair chosen based on the band-limited metric defined in Eq. (7) is stable and does not show the effect of spillover at high frequencies.

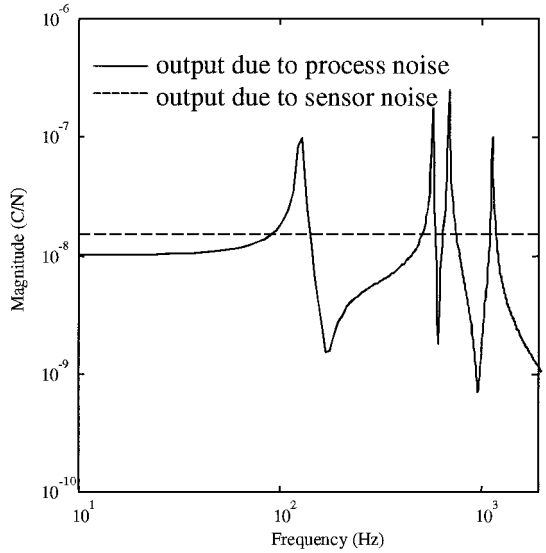

Fig. 6 Magnitude of process noise and sensor noise used in the LQG design.

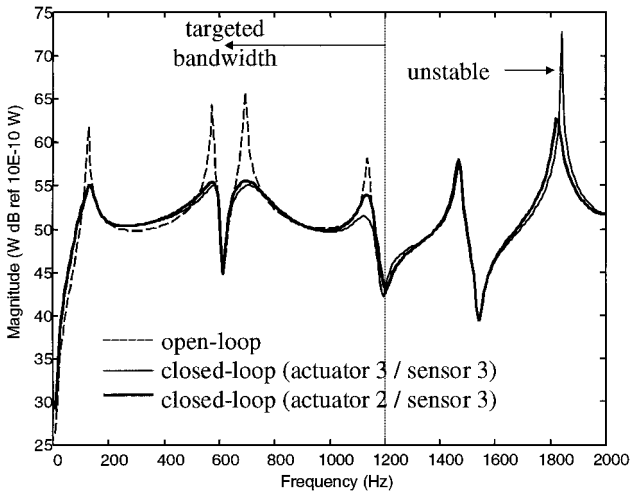

Fig. 7 Magnitude of the closed-loop response for the two alternative transducer pairs selected.

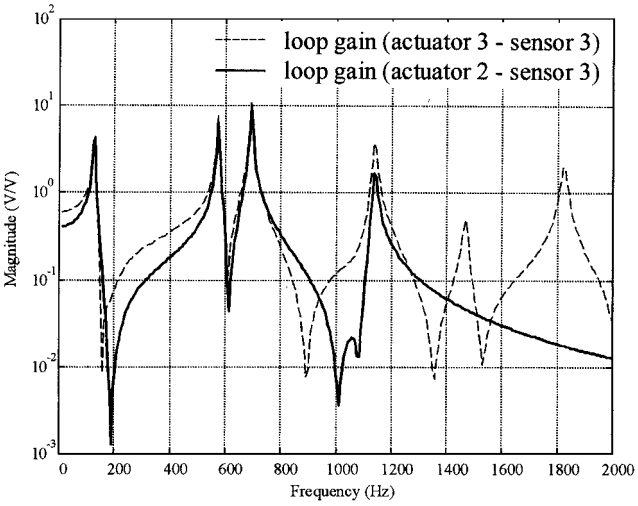

Fig. 8 Loop-gains for actuator 3/sensor 3 [Eq. (4)] and actuator 2/sensor 3 [Eq. (7)].

These results can be anticipated by looking at the loop-gain for each system, presented in Fig. 8. As illustrated, below 1200 Hz, the loop-gains are roughly the same; however, above 1200 Hz, the loop-gain through the collocated transducer pair (actuator 3/sensor 3) is much higher because of significant contribution from out-of-bandwidth modes, exceeding unity at approximately 1838 Hz, resulting in the unstable frequency shown in Fig. 8. The loop-gain associated with the noncollocated transducer pair (actuator 2/sensor 3) above 1200 Hz is much less than unity, explaining the reduced spillover seen in its closed-loop response. This is a result of the spatial filtering in the open-loop plant, achieved by the transducer placement associated with the band-limited metric of Eq. (7). The natural roll-off in frequency response resulting from the metric imposed by the band-limited disturbance rejection actuator selection metric of Eq. (7) resulted in small loop-gains out of the desired bandwidth identified for structural acoustic control, leading to a stable compensator based on a reduced-order model of the system.

Conclusions

A band-limited actuator/sensor selection methodology for disturbance rejection was outlined. Unlike prior methods, which emphasized disturbance rejection in selecting transducers that couple best to modes present in the performance path, the proposed methodology serves to further impose a penalty on the selection of transducer pairs that couple well to modes beyond the identified bandwidth of interest, creating a natural roll-off in the frequency response from the selected spatial apertures of the transducers. Adding the band-limited metric of Eq. (6) to the disturbance rejection metric of Eq. (4) provides the control system engineer with a very powerful method of selecting transducers for feedback control including both disturbance rejection and robustness to model uncertainty outside of the identified bandwidth of interest. For the structural acoustic example provided, a single transducer pair was selected from a possible choice of 49 transducer pairs for reducing the sound power radiated. Although both the disturbance rejection selection method of Eq. (4) and the band-limited disturbance rejection method of Eq. (7) resulted in transducer pairs with very similar performance over the identified bandwidth (<1200 Hz), the band-limited disturbance rejection selection method further resulted in a transducer pair that coupled poorly to structural modes outside of the identified bandwidth of interest. This selection methodology provides the control system engineer with a crude means of introducing loop-shaping concepts in the open-loop plant through the actuator/sensor selection.

References

[1]Gawronski, W., and Lim, K. B., "Balanced Actuator and Sensor Placement for Flexible Structures," *International Journal of Control*, Vol. 65, No. 1, 1996, pp. 131–145.

[2]Lim, K. B., and Gawronski, W., "Hankel Singular Values of Flexible Structures in Discrete Time," *Journal of Guidance, Control, and Dynamics*, Vol. 19, No. 6, 1996, pp. 1370–1377.

[3]Lim, K. B., "Disturbance Rejection Approach to Actuator and Sensor Placement," *Journal of Guidance, Control, and Dynamics*, Vol. 20, No. 1, 1997, pp. 202–204.

[4]Lim, K. B., Lake, R. C., and Heeg, J., "Effective Selection of Piezoceramic Actuators for an Experimental Flexible Wing," *Journal of Guidance, Control, and Dynamics*, Vol. 21, No. 5, 1998, pp. 704–709.

[5]Vipperman, J. S., and Clark, R. L., "Implications of Using Colocated Strain-Based Transducers for Active Structural Acoustic Control," *Journal of the Acoustical Society of America* (to be published).

[6]Clark, R. L., Saunders, W. R., and Gibbs, G. P., *Adaptive Structures: Dynamics and Control*, Wiley, New York, 1998, pp. 376–393.

[7]Gibbs, G. P., Clark, R. L., Cox, D. E., and Vipperman, J. S., "Radiation Modal Expansion: Application to Active Structural Acoustic Control," *Journal of the Acoustical Society of America* (submitted for publication).